

# A Multisite Neural Probe with Simultaneous Neural Recording and Drug Delivery Capabilities

Dhonam Pemba, and William C. Tang, *Senior Member, IEEE*

**Abstract**— This paper presents a novel method for fabricating silicon based planer microelectrodes with SU-8 embedded fluidic channels. A 7 mm long neural probe was fabricated with a 5 mm penetrating shank and a 2mm x 2mm base. One surface of the probe consists of eight 160  $\mu\text{m}$  diameter wire bonding pads connected to eight 60  $\mu\text{m}$  diameter electrode sites on 500  $\mu\text{m}$  centers with eight 15  $\mu\text{m}$  wires interconnects. On the opposite surface lies a 200  $\mu\text{m}$  SU-8 embedded fluidic channel. The fluidic channel was constructed by utilizing two wavelengths of ultraviolet light: a higher wavelength ( $>365\text{nm}$ ) that penetrates the SU-8 completely to construct the fluidic channel walls and a lower wavelength ( $<320\text{ nm}$ ) that only penetrates the surface ( $<60\text{ }\mu\text{m}$ ) to fabricate the roof. The design was chosen for brachial plexus nerve implantation; however, since it was developed using photodefinable processes, the design can easily be adjusted for various applications.

## I. INTRODUCTION

Neural implants aim to interact with the nervous system in hopes of restoring sensory, motor, or cortical functions that can improve or maintain the health of individuals. The electrode is a key component of the neural interface system that records from and/or stimulates neurons. Intraneural electrodes show the most promise for potential use in neuroprosthetic system because they have highest selectivity and signal to noise, with the least cross talk.

Microelectromechanical Systems (MEMS) have allowed intraneural microelectrodes to evolve from single electrodes to precisely definable multisite microelectrodes. Although highly successful in acute settings, the limitation of current electrodes for chronic recording beyond a year has been a barrier to their progress. The natural defense mechanisms of the human body prevent the long term viability of the implants. Initial mechanical trauma from implantation causes an acute inflammatory response with edema, tissue inflammation, and cellular encapsulation of implant[1]. The acute response is followed by a chronic foreign body reaction several weeks later that includes macrophage glial scarring and fibrotic encapsulation[2]. A multisite neural electrode with fluidic delivery capabilities could not only prevent these reactive cellular responses[3], but also allow for electrophysiological measurements[4] and the capability to delivery drugs that enhance nerve regeneration[5]

Dhonam Pemba is with the Biomedical Engineering Department, University of California, Irvine, CA, 92697 USA (corresponding author; phone: 949-214-9738; email: dpemba@uci.edu).

William C. Tang is with the Biomedical Engineering Department, University of California, Irvine, CA, 92697 USA

Within the last decade there have been efforts to include fluidic channels in electrodes. Several neural probes with fluidic delivery capabilities have been fabricated with methods that include sealing[4], bonding[6,7] and sacrificial spacers[8,9]. The channel depth and deliverable volume is limited by the small opening needed for sealing and/or the thickness of the sacrificial material. While bonding, is susceptible to leakage and misalignments.

We present a novel alternative to all the previously attempted methods of creating fluidic microelectrodes. The method presented uses well established MEMS processes that allow for scalability, reproducibility, and precision dimension control. The neural electrodes consist of a silicon shank, with electrode sites, and an embedded fluidic channel constructed out of SU-8.

## II. DESIGN

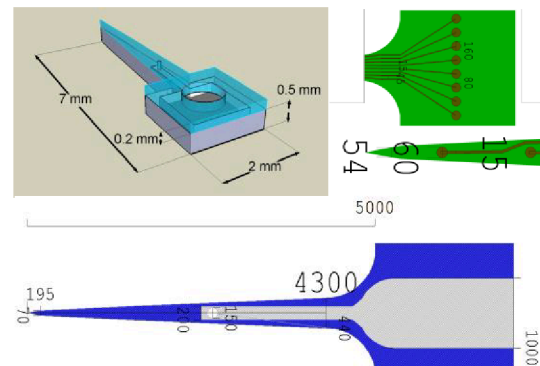


**Figure 1:** Three Dimensional schematic with a 500  $\mu\text{m}$  silicon substrate and 200  $\mu\text{m}$  thick embedded SU-8 microchannel layer (Top Left), Electrode layout- eight 160  $\mu\text{m}$  diameter wire bonding pads connected to eight 60  $\mu\text{m}$  diameter electrode sites on 500  $\mu\text{m}$  centers with eight 15  $\mu\text{m}$  wires interconnects (Top Right), Top view schematic with 200  $\mu\text{m}$  channel with 150  $\mu\text{m}$  outlet and 1mm inlet (Bottom).

The fluidic neural probes were designed for upper limb motor neuroprostheses. An electrode array would stimulate and/or record from both efferent and afferent nerves in the brachial plexus. Efferent signals of motor intention can be amplified, digitized, and processed to control an artificial arm or limb, while electrodes could stimulate afferent signals to transmit proprioceptive and sensory information to the brain, where the cerebellum can process adjustments and transmit them to the motor cortex. Nerves in the brachial plexus range from 0.7 to 9 mm in diameter, we decided to design the electrodes to fit the cervical nerves of the brachial plexus where the average diameter is about 5 mm[10] (Figure 1). The penetrating shank of the probe is 5 mm long

and connects to a 2 mm x 2 mm base. In order to increase the mechanical strength of the shank, it is curved into the base instead of a linear taper (not depicted in three dimensional rendering in Figure 1). The base of the shank begins to curve at 700  $\mu\text{m}$  from the base. The  $10.18^\circ$  angle of inclination from the medial was designed to be less than  $20^\circ$  to mitigate potential trauma from insertion[11]. Eight 150  $\mu\text{m}$  diameter wire bonding pads were connected to eight 60  $\mu\text{m}$  diameter electrode sites on 500  $\mu\text{m}$  centers with eight 15  $\mu\text{m}$  wires separated by 25  $\mu\text{m}$ .

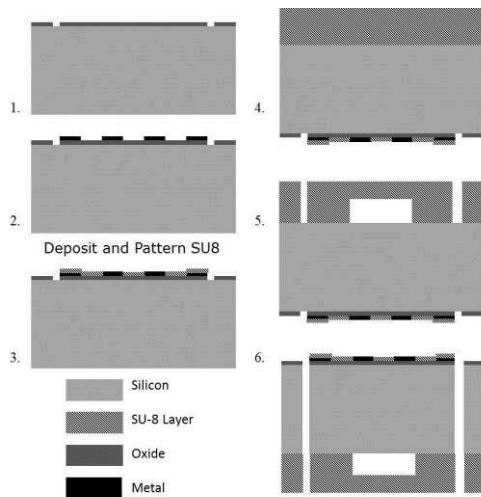


**Figure 2:** Fabrication Flow- Pattern metal on oxide (1-2), Pattern SU-8 dielectric over electrodes and interconnect(3), Create embedded SU-8 microchannel on backside(4-5), Etch and release probes with Deep Reactive Ion Etching(6)

### III. FABRICATION

The fabrication of the topside electrode interconnects, traces, bonding pads, and dielectrics are illustrated in Figure 2. First, 0.5  $\mu\text{m}$   $\text{SiO}_2$  was grown under thermal oxidation at  $1100^\circ\text{C}$  to insulate the electrodes. Next, gold pads, electrode sites, traces, and interconnects were patterned via lift off (Shipley 1827 3500 RPM, 30 seconds, acceleration 500 rpm/s, 10 minute bake at  $95^\circ\text{C}$ ,  $220 \text{ mJ}/\text{cm}^2$  exposure on Karl Suss MA6 Mask Aligner, 50 seconds development using Microposit MF-319, 20 nm Ti/ 150 nm Au). Finally, 2  $\mu\text{m}$  of SU-8 were patterned to serve as the top dielectric.

After the electrode interconnects were fabricated, the fluidic channel on the reverse side was constructed.

#### *The fabrication of embedded SU-8 microchannels*

There is a well-established phenomenon known as “T-topping” that occurs with SU-8, where the top corners overhang[12]. T-topping occurs due to low optical transmittance of SU-8 for wavelengths below 350 nm as these wavelengths cannot penetrate beyond the surface of SU-8. The manufacturer of SU-8, Microchem Inc., suggests using a filter to eliminate wavelengths below 350 nm to obtain vertical sidewall profiles. However, instead of eliminating the lower wavelength light, it could be used to our advantage in sealing microchannels. The embedded

microchannels were fabricated by first spinning 2  $\mu\text{m}$  of SU-8 2002 to increase adhesion and reduce delamination. Next, 180  $\mu\text{m}$  of SU-8 2050 was spun on the wafer. The first exposure with the 365 nm unfiltered light defined the channel walls and probe shape ( $400 \text{ mJ}/\text{cm}^2$ ). The wafer was baked at 10 minutes at  $65^\circ\text{C}$ , 10 minutes at  $80^\circ\text{C}$ , 20 minutes at  $90^\circ\text{C}$ , then cooled gradually for 10 minutes at  $80^\circ\text{C}$ , 10 minutes at  $65^\circ\text{C}$ . Finally, the hotplate was turned off to allow the wafer to reach room temperature. Next, the channel roof, inlet, outlets, and probe shape were patterned with exposure to UV light filtered by the 312 nm band pass filter ( $480 \text{ mJ}/\text{cm}^2$ ). Figure 3 depicts a cross-sectional view of this process.

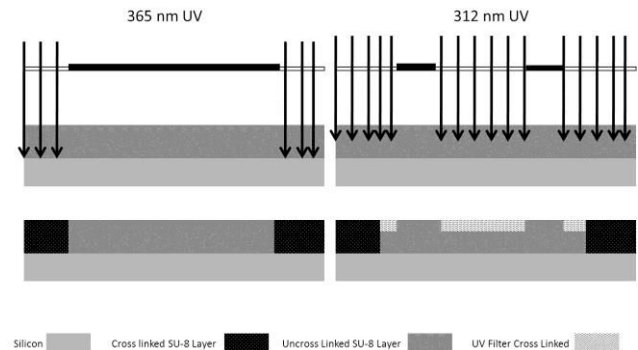


**Figure 3:** Varying wavelengths of light used to create the embedded microchannel. Ultraviolet light with wavelengths  $> 365 \text{ nm}$  transmits completely through the SU-8 to define channel walls. Lower wavelength light at 312 nm seals the channels and defines inlets and outlets ports.

#### *Topside Probe Release*

Once the channel was fabricated on the backside, the opposite side was patterned to define the probe shape. 15  $\mu\text{m}$  AZ 4620 photoresist (1000 RPM, 1 minute acceleration at 500 rpm/s, 20 minute baking at  $95^\circ\text{C}$ ,  $600 \text{ mJ}/\text{cm}^2$  exposure on Karl Suss MA6 Mask Aligner, 5 minutes development using 1:3 AS400K:H2O). Next, the device wafer was mounted to a 500  $\mu\text{m}$  thick handle wafer using photoresist and thermal grease. Photoresist was spun on the edge of the handle wafer and thermal grease was added to the device wafer while avoiding the devices. The two wafers were brought in contact and placed in a  $90^\circ\text{C}$  for 40 minutes. The initial oxide was patterned using Trion (150mT, RIE RF 100W,  $\text{CF}_4$  45 sccm,  $\text{O}_2$  5 sccm, He pressure 5mT, etch time 20 minutes). The patterned photoresist and oxide defined the mask for Deep Reactive Ion Etching (DRIE) etching. The wafer was etched in Surface Technology Systems DRIE system until each probe separated (approximately 165 minutes). The probes were soaked in acetone for 30 minutes, then isopropanol for 2 days to remove photoresist, and finally 10 minutes in ultrasonic bath to remove any residual photoresist.

#### IV. RESULTS

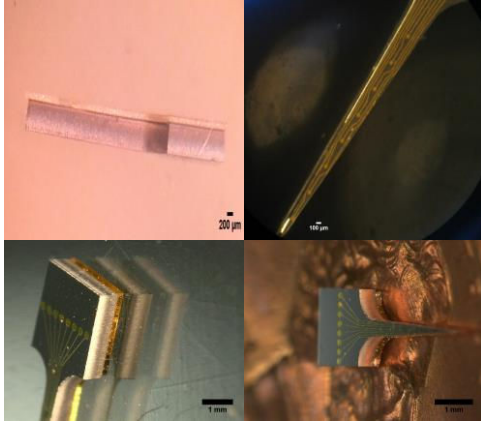


**Figure 4:** Results of fabricated probes. Side view of fabricated probe(Top Left), Precisely defined electrodes(Top Right), Bonding pads(Bottom Left), Fabricated probe pictured on top of a penny(Bottom Right)

Several hundred prototypes 7 mm long multielectrodes were fabricated with a 5 mm penetrating shank and a 2 mm x 2 mm base. One surface of the probe consists of eight 160  $\mu\text{m}$  diameter wire bonding pads connected to eight 60  $\mu\text{m}$  diameter electrode sites on 500  $\mu\text{m}$  centers with eight 15  $\mu\text{m}$  wires interconnects. On the opposite surface lies a 200  $\mu\text{m}$  SU-8 embedded fluidic channel. Figure 4 depicts photos taken of the fabricated probes. The current design and fabrication process yields over 70 multielectrodes from one 4 inch wafer.

##### 1) Channel Testing

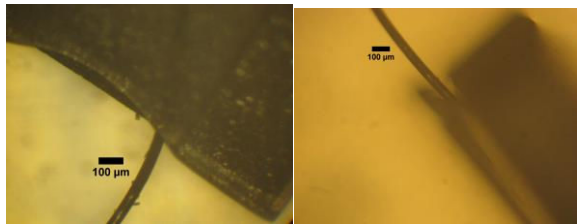


**Figure 5:** Wire inserted into the inlet of the fluidic multielectrode

The presence of a channel was checked visually and mechanically by inserting a 50  $\mu\text{m}$  into the inlet (Figure 5), and by pumping dye through the channel (Figure 6). In order to characterize the channel flow for probes fabricated with our method, we designed fluidic test channels. The fabrication procedure was identical to our process, but the dimensions differed in length and width. Four 10 mm channels of 200  $\mu\text{m}$ , 300  $\mu\text{m}$ , 400  $\mu\text{m}$ , and 500  $\mu\text{m}$  widths were fabricated. A 100  $\mu\text{l}$  pipette filled with 1% blue dye was put in contact with the channels and capillary action drove the fluid to the outlet (Figure 7). The velocity of fluid movement via diffusion from capillary forces was measured to range from 50 mm/s (200  $\mu\text{m}$  wide channel) to 60mm/s (500  $\mu\text{m}$  wide channel). These results suggest once drugs are pumped into the channel, they should be released quickly.

Structural strength was investigated by penetrating a frog's sciatic nerve and PDMS(Figure 8). The Young's

modulus of a peripheral nerve is about 600 kPa[13] and the modulus of PDMS is about 1MPa[14]. Figure 8 demonstrates that the electrodes could penetrate both the nerve and a stiffer PDMS without any structural damage.

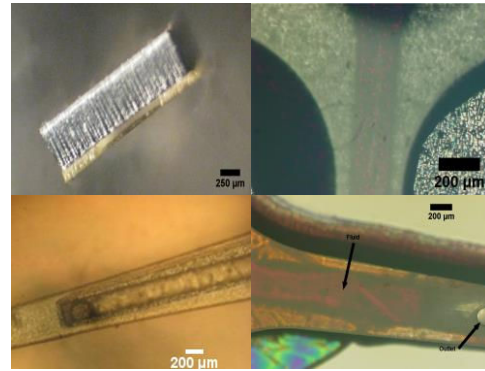


**Figure 6:** Embedded microchannel. Fluidic inlet(Top Left), Red dye pumped in channel(Top and Bottom Right), Fluidic outlet(Bottom Left)

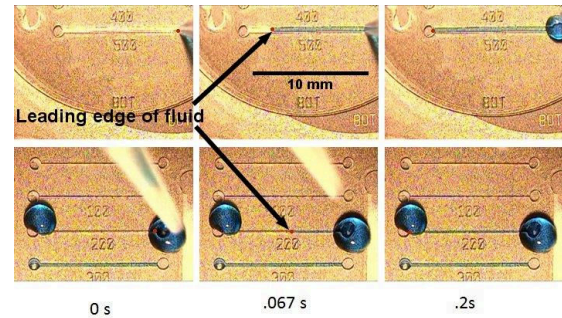


**Figure 7:** Fluidic channel velocity test- blue dye moving through a 500  $\mu\text{m}$  width channel (Top), blue dye moving through a 200  $\mu\text{m}$  width channel (Bottom), the large bubble on the left of the 200  $\mu\text{m}$  width channel was not part of the test (Bottom).



**Figure 8: Mechanical test.** Insertion of electrode in frog's sciatic nerve (Left), Insertion through PDMS(Right).

##### 2) Electrical Test

The electrical impedance in 0.9 % saline was measured using a standard three cell configuration. Sine waves from 10 Hz to 1 MHz was passed through neural electrode and Pt counter electrode. The current was measured across a 1 k $\Omega$  resistor. The voltage drop measured between the neural electrode and a Pt reference electrode was divided by the current to obtain impedance. Impedance was between 500 k $\Omega$  to 800 k $\Omega$  which was within range of other microelectrodes[15].

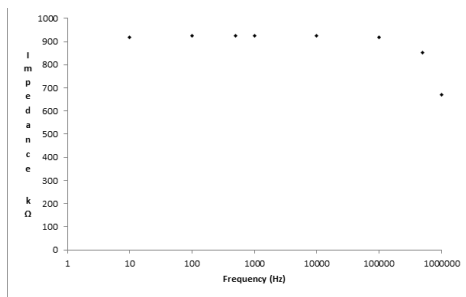


**Figure 9:** Stimulating and recoding testing. Stimulating electrode on channel 1, recording electrode on channel 2

## V. CONCLUSION

This paper has described the design, characterization, fabrication, and testing methods of a neural electrode with simultaneous fluidic delivery and electrical capabilities. The fabrication process discussed above was designed to rely only on MEMS based processes which allows for precise dimensional control. Although the work presented here was fabricated for applications in brachial plexus nerve, the fabrication procedure could easily be adapted to other parts of the nervous system including smaller nerves and the cortex. All of the processes used in fabrication are dependent on photolithography, and therefore other geometrical configurations can be readily produced by modifying the photomask design.

## ACKNOWLEDGMENTS

The author would like to thank Tina Zhu, Christopher Tu and Andrea Navarro for their assistance. The author acknowledges support from the staff of the Integrated Nanosystems Research Facility and the Laboratory for Electron and X-ray Instrumentation

## REFERENCES

- [1] S. S. Stensaas and L. J. Stensaas, "The reaction of the cerebral cortex to chronically implanted plastic needles," *Acta neuropathologica*, vol. 35, no. 3, p. 187, 1976.
- [2] D. H. Szarowski, M. D. Andersen, S. Retterer, A. J. Spence, M. Isaacson, H. G. Craighead, J. N. Turner, and W. Shain, "Brain responses to micro-machined silicon devices," *Brain research*, vol. 983, no. 1, pp. 23–35, 2003.
- [3] S. T. Retterer, K. L. Smith, C. S. Bjornsson, K. B. Neeves, A. J. H. Spence, J. N. Turner, W. Shain, and M. S. Isaacson, "Model neural prostheses with integrated microfluidics: A potential intervention strategy for controlling reactive cell and tissue responses," *IEEE Transactions on Biomedical Engineering*, vol. 51, no. 11, pp. 2063–2073, 2004.
- [4] J. Chen, K. D. Wise, J. F. Hetke, and S. C. Bledsoe, "A multichannel neural probe for selective chemical delivery at the cellular level," *IEEE transactions on bio-medical engineering*, vol. 44, no. 8, pp. 760–9, Aug. 1997.
- [5] J. Fallon, S. Reid, R. Kinyamu, I. Opole, R. Opole, J. Baratta, M. Korce, T. L. Endo, A. Duong, and G. Nguyen, "In vivo induction of massive proliferation, directed migration, and differentiation of neural cells in the adult mammalian brain," *Proceedings of the National Academy of Sciences*, vol. 97, no. 26, pp. 14686–14691, 2000.
- [6] K. Seidl, S. Spieth, S. Herwik, J. Steigert, R. Zengerle, O. Paul, and P. Ruther, "In-plane silicon probes for simultaneous neural recording and drug delivery," *Journal of Micromechanics and Microengineering*, vol. 20, no. 10, p. 105006, Oct. 2010.
- [7] A. Altuna, "SU-8 BASED MICROPROBES FOR SIMULTANEOUS NEURAL DEPTH RECORDING AND DRUG DELIVERY IN THE BRAIN," *Lab on a Chip*, 2013.
- [8] D. Kipke and D. Pellinen, "Flexible polymer microelectrode with fluid delivery capability and methods for making same," *US Patent App. 11/452,551*, 2006.
- [9] K. B. Neeves, C. T. Lo, C. P. Foley, W. M. Saltzman, and W. L. Olbricht, "Fabrication and characterization of microfluidic probes for convection enhanced drug delivery," *Journal of controlled release : official journal of the Controlled Release Society*, vol. 111, no. 3, pp. 252–62, Apr. 2006.
- [10] H. Y. Lee, I. H. Chung, W. S. Sir, H. S. Kang, H. S. Lee, J. S. Ko, M. S. Lee, and S. S. Park, "Variations of the ventral rami of the brachial plexus," *Journal of Korean medical science*, vol. 7, no. 1, p. 19, 1992.
- [11] D. J. Edell, V. V. Toi, V. M. McNeil, and L. D. Clark, "Factors influencing the biocompatibility of insertable silicon microshafts in cerebral cortex," *Biomedical Engineering, IEEE Transactions on*, vol. 39, no. 6, pp. 635–643, 1992.
- [12] S. J. Lee, W. Shi, P. Maciel, and S. W. Cha, "Top-edge profile control for SU-8 structural photoresist," in *University/Government/Industry Microelectronics Symposium, 2003. Proceedings of the 15th Biennial, 2003*, pp. 389–390.
- [13] G. H. Borschel, K. F. Kia, W. M. Kuzon Jr, and R. G. Dennis, "Mechanical properties of acellular peripheral nerve," *Journal of Surgical Research*, vol. 114, no. 2, pp. 133–139, 2003.
- [14] D. Fuard, T. Tzvetkova-Chevolleau, S. Decossas, P. Tracqui, and P. Schiavone, "Optimization of poly-di-methyl-siloxane (PDMS) substrates for studying cellular adhesion and motility," *Microelectronic Engineering*, vol. 85, no. 5, pp. 1289–1293, 2008.
- [15] S. F. Cogan, "Neural stimulation and recording electrodes," *Annual review of biomedical engineering*, vol. 10, pp. 275–309, Jan. 2008.